The Relation Between Foundation Embedment and Peak Horizontal Input Acceleration: The Case of Strip Foundation with Partial Contact to Surrounding Medium

Hossein Jahankhah[1] and Pouran Fallahzadeh[2]*

1. Assistant Professor, Geotechnical Engineering Research Center, International Institute of Earthquake Engineering and Seismology (IIEES), Tehran, Iran,
* Corresponding Author; email: h.jahankhah@iiees.ac.ir
2. PhD Student, International Institute of Earthquake Engineering and Seismology (IIEES), Tehran, Iran

ABSTRACT

In the field of soil-structure interaction (SSI), kinematic interaction (KI) can potentially be a source of notable influence on dynamic response. Such influence takes place through alternation in free field motion (FFM) and results in new foundation input motions (FIM). In this paper, first, the effect of KI on horizontal input motion for the case of single rigid strip embedded foundation with incomplete contact between sidewall and nearby soil under vertical propagation of shear waves is investigated. Then, it is discussed that how this input-change would be reflected in peak horizontal input acceleration (PHIA). Results for different embedment depths and various soil-wall contact lengths are depicted. In this research, numerical analysis was conducted by ABAQUS finite element software. It is shown that the effects of kinematic interaction are significant for high frequencies of excitation. Besides, it is illustrated that foundation shape and its contact area to surrounding soil alter the PHIA usually conservatively with some exceptions in the case of zero contact lengths.

1. Introduction

A realistic evaluation of dynamic response of structure requires consideration of soil structure interaction. Inertial and kinematic interactions are two major issues that should be considered when base flexibility is introduced to dynamic analysis. Among these two, KI is the phenomenon that would alter the FFM to new foundation input motions. This alternation usually modifies the frequency content and even may become a source to generate a set of input motions in new degrees of freedom [1-2]. A well-known example of the above phenomenon is the reduction in horizontal amplitude and inducing rocking input motion to embedded foundation under vertical propagating shear waves

[3-4]. According to previous findings, KI would be affected by different parameters like properties of soil, shape and embedment depth of foundation, besides type and angle of inclined waves [5-7]. Thus, because of peculiar importance of this issue in seismic structural analysis, many researchers have addressed this subject in recent decades. An approximate analytical solution was developed by Novak [8-9] to predict the foundation dynamic response. Then, the introduced Analytical solution was compared with finite element and field experiment result. KI effects on embedded rectangular foundation were formulated and examined using field data by Hoshiya [10]. Iguchi [11] estimated

dynamic response of cylindrical foundation due to variation of foundation embedment depth and incident wave angle. Dynamic response of circular foundation excited by non-vertically propagating SH, SV, P and also Rayleigh waves was reported by Luco and Mita [12]. Further, Luco [13] presented the torsional response of a rigid hemispherical foundation excited by an obliquely incident plane SH wave. Input motion of rectangular foundation excited by obliquely propagating shear wave was investigated by Wong and Luco [14] and revealed the marked effect of seismic wave incidence angle on FIM. Moreover, Luco and Wong [15] explored the input motion of embedded foundation by an integral equation technique. In the other research, Mita and Luco [16] presented the response of square embedded foundation by hybrid method. They reported that the response of square foundation can be approximated by that of cylindrical foundation with an equivalent circular base and the same embedment depth. Besides, Input motion of square foundation due to vertical shear and compression waves tabulated parametrically by Mita and Luco [17]. Veletsos and Prasad [18] reported the effect of incident incoherent wave field on circular massless-foundation response. KI is usually quantified by transfer function (TF), which is the ratio of FIM components to FFM in frequency domain. Embedment depth is a crucial parameter to calculate the mentioned transfer function. Results demonstrated that the deeper foundation would experience intensified rocking and diminished horizontal input motions [1, 9]. Kausel [19] investigated the response of embedded rectangular foundation, resting on homogenous soil with damping ratio of 5%, by direct finite element and substructure method. He compared the results extracted from these two methods. To compare previously proposed approximate method with experimental results, Kurimoto and Iguchi [20-21] conducted extensive shaking table tests on KI of embedded foundation. They reported good agreement between two implemented methods. Givens [22], through reliable empirical investigation on real databases, has reported kinematically induced FIMs. The empirical results were then compared to existing approximations. The results uncover conservatism aspects of current practise in low frequencies and underestimation for the rest. In the same research,

experimental tests using centrifuge and shaking table devices were conducted to investigate the beneficial and detrimental effects of KI. These researches are utilized as benchmarks for crosscheck of analytical analysis [23, 24].

2. State of the Problem

As mentioned before, the order of KI effects depends on different parameters. Although the importance of foundation characteristics, especially embedment depth, to determine FIM was discussed widely, one of notable points, which is contact length of foundation side-wall to surrounding soil, has not been considered comprehensively yet. The other significant point, which has not attracted enough attentions in spite of its engineering prominence, is the influence of KI on the PHIA imposed to foundation. For instance, in common seismic hazard analysis procedures, estimating PGA is one of the important issues. The calculated accelerations in such procedures, without any change, are sometimes implemented in design routines. That's while the seismic peak horizontal acceleration experienced by any system, even before introducing mass of super structure to the problem, would differ from PGA just as a matter of KI effects.

In this paper, first, the effect of KI on input motion for the case of single strip embedded foundation with incomplete contact between side-wall and nearby soil under vertical propagation of shear waves is investigated. Then, it is discussed that how this input-change would be reflected in PHIA experienced at the bottom of foundation.

3. Modelling and Validation

The model details and its parameters are illustrated in Figure (1a), in which *D* is embedment depth, *d* is contact length and a is half-width of the foundation.

Numerical analysis is conducted by ABAQUS finite element software [25] to extract the transfer function (TF) components of kinematically induced input motions. This simulation was two-dimensional and done for strip foundation subjected to vertical propagating field of shear wave. Figure (1b) depicts schematically the sample deformed shape at an arbitrary time and input pulse inserted at the base of the model. The well-known free field columns at
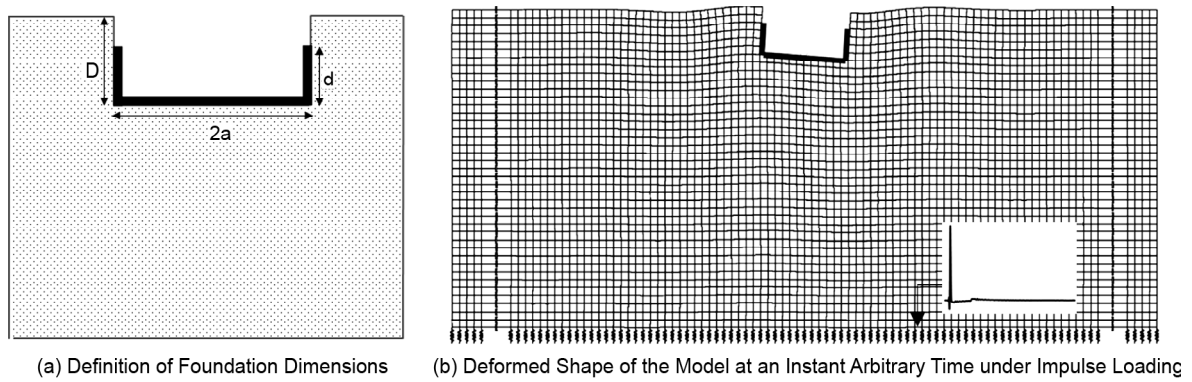
(a) Definition of Foundation Dimensions

(b) Deformed Shape of the Model at an Instant Arbitrary Time under Impulse Loading

Figure 1. Description of the model.

sides of the model are used to simulate 1D propagation of shear wave field. Such columns are attached to the main middle part of the model through viscous elements that along with viscoelastic boundaries at the base have provided an integrated transmitting boundary condition in the perimeter.

Validation of the model is an important part of simulation to examine the accuracy of the results. In this regard, as a sample, the horizontal impedance functions along with the kinematically induced translational FIM for the case of full contact state is compared to past findings, which are defined as benchmarks in this field [4, 26]. Figures (2a) and (2b) represent the horizontal impedance functions calculated in this research compared with the ones calculated by Wang [26] using boundary element method. The vertical axis of the mentioned figures shows dynamic stiffness and damping respectively. The horizontal axis shows non-dimensional frequency of excitation, $a_0 = \omega * a / Vs$ where ω is frequency of excitation and Vs is shear wave velocity of the medium. As can be seen in the whole frequency range, in spite of using different methods, a reasonable match is achieved for both stiffness and damping graphs. A further cross check is conducted for the case of horizontal foundation input motion in Figure (2c). In this figure, the resulted kinematically induced horizontal TF in current study is examined against similar results reported by Pais [4] using an approximate method. This figure shows the amplitude ratio of horizontal foundation input motion to FFM versus a_0. This comparing graph illustrates the same trend and reveals appropriate simulation. The minor deviation between results seems to be originated from the benchmark approximations as was emphasized by
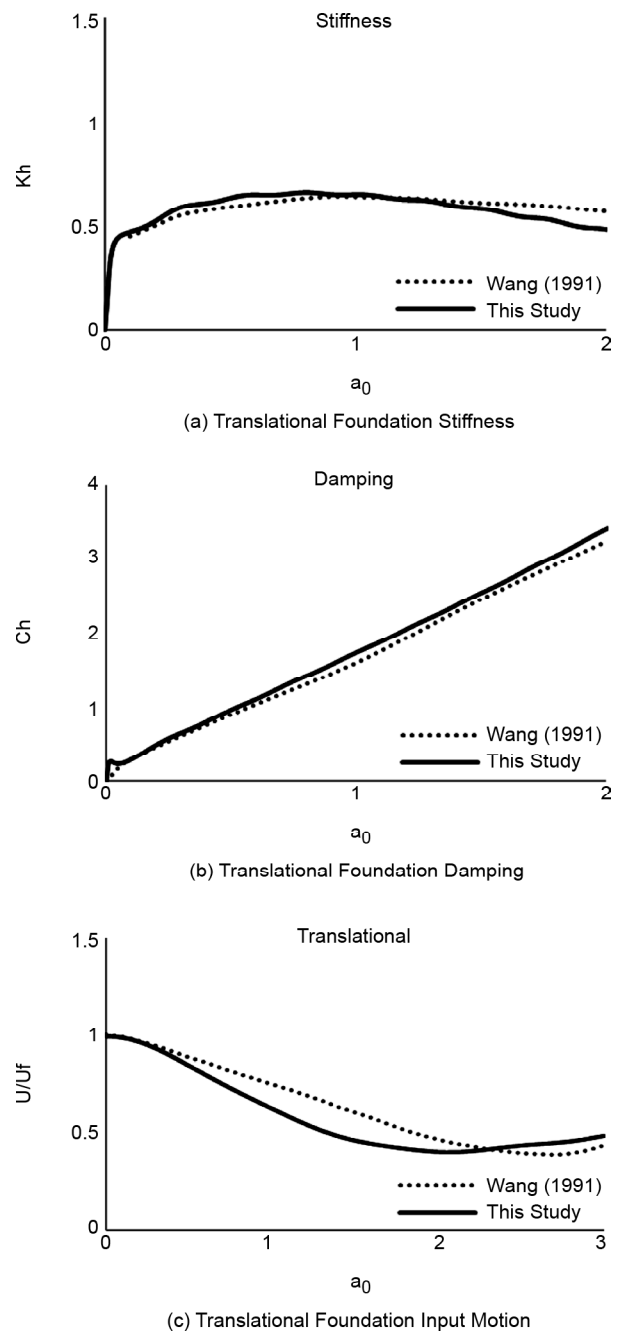

(a) Translational Foundation Stiffness

(b) Translational Foundation Damping

(c) Translational Foundation Input Motion

Figure 2. Comparing results from this study to that of Benchmarks [4, 26].

the author [4].

Table (1) represents the soil properties and foundation dimensions of this validation test.

It should be emphasized that, as the results are depicted in a non-dimensional format, they would be applicable for every set of soil properties with $\upsilon = 0.3$ and different dimensions of foundation for which non-dimensional parameters lay within the ranges reported in figures, but not only the ones illustrated in Table (1).

Table 1. Properties of soil and foundation dimensions.

Prop.	υ	ρ	Vs	a	D
	0.3	1.65gr/cm^3	100m/s	3m	3m

In the following parts, the results will be presented for different embedment ratios, D/a. Here, four values of 0.5, 1, 1.5 and 2 are considered for this non-dimensional parameter, which would cover a reasonable range of variations [27]. In addition, in the concluding notes, four contact length ratios of soil-side wall, d/D, are reported that varies between 0, as a symbol of non-contact condition of side-wall to nearby soil, to 1 that is a representative of full contact situation. Two values of 0.25 and 0.5 are also included within the mentioned range as well. The specific state with $D/a = 1$ and $d/D = 1$ was considered for model validation in Figure (2).

4. Method of Analysis

The following procedure was conducted for assessment of KI effects on foundation input motion and PHIA.

1. An instant pulse is implemented at the bottom of the model. Then, FFM and FIM time histories of the foundation under mentioned excitation are extracted from different models, i.e. without and with inclusion of the foundation.
2. Fourier transfer function of translational FIMs is divided by similar ordinates from FFMs. Hence, TFs regarding KI effects are derived.
3. An ensemble of twenty FFM real records is chosen.
4. The time history of records is converted to frequency domain.
5. By product of TF from step 2 and each Fourier

transform of records from step 4, the frequency domain representation of KI induced FIMs from ensemble ground motion is achieved.
6. The frequency domain FIMs of step 5 are converted to time domain.
7. Peak acceleration of resulted horizontal foundation input motions, from step 6, are scaled by PGA of respective FFM.

Following steps 1 to 7, the target set of PHIA to foundation is achieved.

5. Result and Discussion

Analyses were accomplished parametrically and extracted graphs are reported in two successive parts. First part covers frequency domain major aspects of the results, and second part reviews time domain key characteristics, respectively.

5.1. Frequency Domain Aspects of the Results

Figure (3) shows the translational TF components of rigid embedded strip foundation with various contact lengths to soil against a_0. The figure consists of results belonging to different embedment ratios, D/a.

Regarding different characteristics of embedment and contact conditions, the following conclusions may be drawn:

- For all horizontal TFs, by increasing non-dimensional frequency, starting from zero, a decreasing trend from an initial value of unity is witnessed. After that, a non-complete build-up with some fluctuations happens that may hardly cause the ordinate to meet an amount of unity again. Hence, it can be concluded that the KI induced horizontal FIM, scale the amplitude of all components of FFM to a fraction of unity.

- Comparing soil-wall full and partial contact states, show different trends in low and high non-dimensional frequencies. For low values of a_0, before a specific threshold, the state of partial contact reduces amplitudes of horizontal FIM. That's while beyond that limit, a reverse trend takes place in such a way that the ordinate again approaches to unity as the values of a_0 grow up. This tendency intensifies for the state of no soil-wall contact. The mentioned threshold diminishes as the contact length descends and embedment ratio increases.

5.2. Time Domain Characteristics of the Results

The next question is that: "How the above mentioned TFs would affect FFM time histories and related PHIAs?". To answer this question, first, such effects are illustrated on sample records. Figure (4a) shows the time history of two different FFM records, the descriptions of which will later be presented in Table (2). The records entitled R1 and
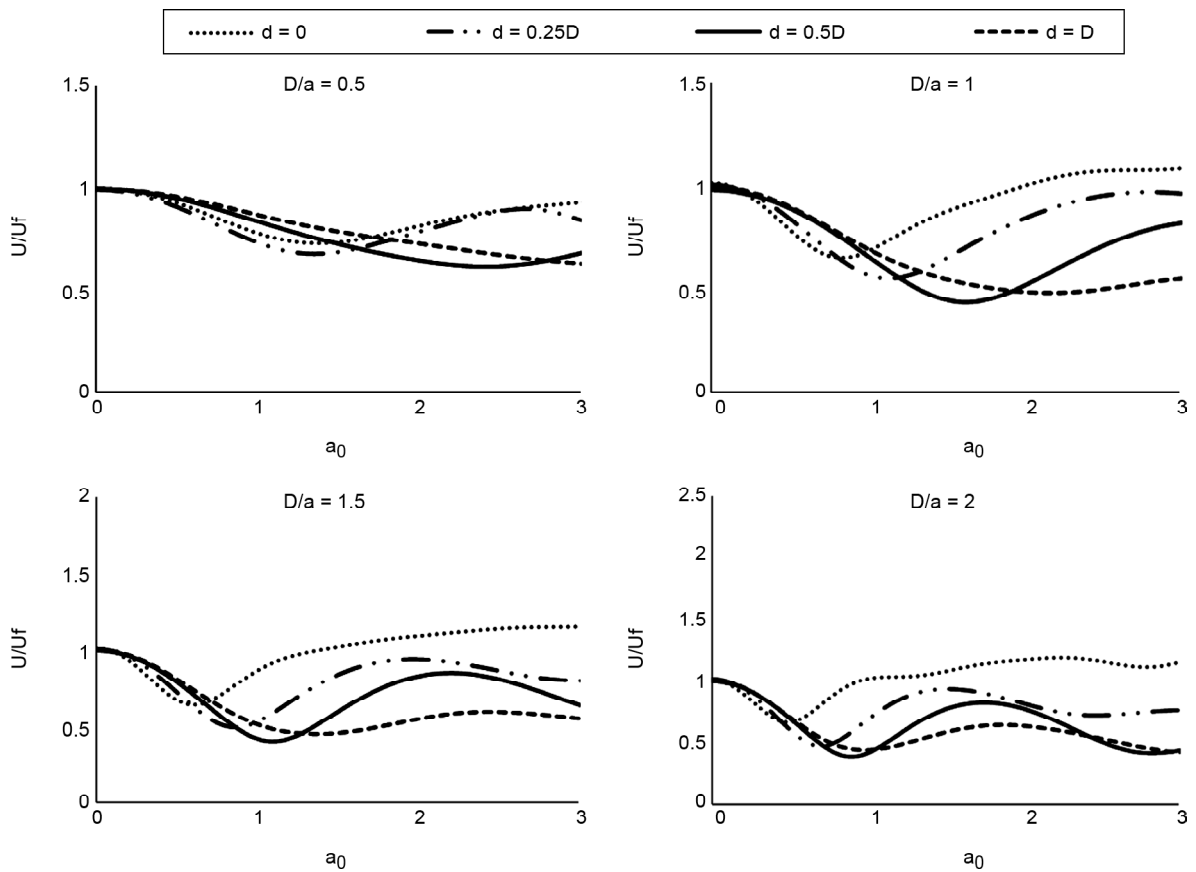
Figure 3. The ordinate ratios of horizontal FIM to FFM in frequency domain arranged by different embedment ratios for various side wall contact lengths to nearby soil.

**Table 2.** Descriptions of real selected records.

Station	Geology	Earthquake Date	Magnitude	Epicentral Distance (km)	Component	PGA (g)
El Centro-Irrigation Distinct	Alluvium	Imperial Valley, May 18, 1940	6.3(ML)	8	S90W, S00E	0.21 0.31(R1)
Taft Lincoln School Tunnel	Alluvium	Kern County, July 21, 1952	7.7(MS)	56	308 , 218	0.15, 0.18
Figueroa 445 Figueroa St.	Alluvium	San Fernando, February 9, 1971	6.5(ML)	41	N52E, S38W	0.14, 0.12
Ave. of the Stars 1901 Ave. of the Stars	Silt and Sand Layers	San Fernando, February 9, 1971	6.5(ML)	38	N46W, S44W	0.14, 0.15
Meloland_ Interstate 8 Overpass	Alluvium	Imperial Valley, October 15, 1979	6.6(ML)	21	360 , 270	0.31, 0.30
Bond Corner Heighways 98 and 115	Alluvium	Imperial Valley, October 15, 1979	6.6(ML)	3	140 , 230	0.51, 0.78
Alhambra Freemont School	Alluvium	Whitter_ Narrows, October 1, 1987	6.1(ML)	7	270 , 180	0.41, 0.30
Altadena Eaton Canyon Park	Alluvium	Whitter_ Narrows, October 1, 1987	6.1(ML)	13	90 , 360	0.15, 0.30
Burbank California Federal Saving Building	Alluvium	Whitter_ Narrows, October 1, 1987	6.1(ML)	26	250 , 340	0.23, 0.19
Holister _ South and Pine	Alluvium	Loma Prieta, October 17, 1989	7.1(MS	48	90 , 180	0.25(R2) 0.21

R2 possess peak acceleration of about 0.31 g and 0.25 g respectively. The records have different frequency content as can be followed in Figure (4b). At the first glance, it can be seen that R1 is much richer in high frequencies rather than R2. Then, these two records are used to derive PHIA for two different foundation-soil contact states. These states are zero and full contact lengths of side-walls to surrounding soil, i.e. $d/D = 0$ and 1. For both cases, D/a is considered to be about 2. As can be seen in figure (4c), for the case of zero contact length, modified R1 record shows notable grow to the value of 0.42 g in peak acceleration. Opposite trend is witnessed for the same record for full contact condition, in Figure (4e), where peak acceleration reduces to 0.16 g. That's while for record

R2, PHIA diminishes by the same order in both states of contact length to the value of 0.19 g. This shows that PHIA is highly dependent to frequency content of original record. For the above cases, Figures (4d) and (4f) show how KI would affect frequency content of FFM records.

To provide more comprehensive engineering insight to PHIA variation under kinematic interaction, an ensemble of ground motions consists of 20 records, including the previously introduced records, R1 and R2, is investigated in this research. The descriptions of mentioned records are listed in Table (2).

The calculated PHIAs are normalized to PGA of respective FFM records and plotted against different ratios of Vs/a. This later parameter is
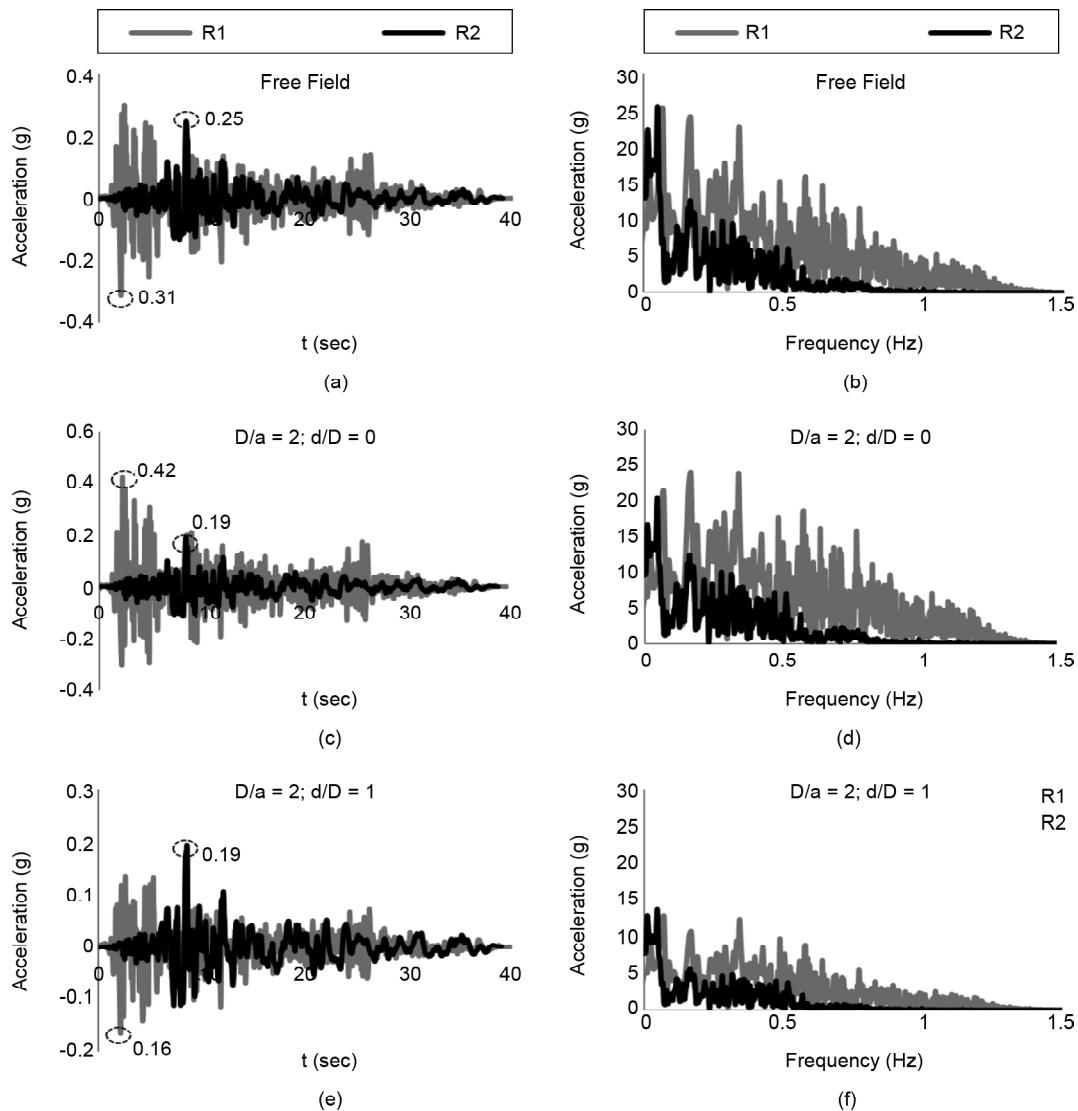
Figure 4. Effect of KI on two sample FFM real records, Vs/a=10:(a, b) FFM records and respective Fourier transforms, (c,d) horizontal FIMs for the case D/a=2, d/D=0 and respective Fourier transforms, (e, f) horizontal FIMs for the case D/a=2, d/D=1 and respective Fourier transforms.

considered to variate from 10 to 100. In practice, rarely one would encounter a case that takes values less than the above lower bound, i.e. 10, for Vs/a. But for the upper bound, i.e. 100, larger values may often take place. Results are depicted in Figure (5) that consists of a matrix of charts with four rows and four columns. The variations of foundation embedment depth and soil-wall length states are expressed in rows and columns respectively. Each chart belongs to specific value of d/D and D/a ratios. In every chart, first, results for 20 records are presented in grey style together. Then, the graphs of average (μ), average plus standard deviation ($\mu+\sigma$) and average minus standard deviation ($\mu-\sigma$) are highlighted over basic ensemble results by thick black and red curves respectively. Four values of 0, 0.25, 0.5, and 1 are considered for contact length ratios. Moreover, four embedment ratios of 0.5, 1, 1.5, and 2 are considered in present study.

With respect to the PHIA graphs, in different conditions of embedment depth and soil-wall contact length ratios, following points can be figured out:

- KI could affect PHIA drastically. The influence level is generally intensified as D/a grows up.
- For $d/D=1$, this effect is in the conservative side, that at most reduces PHIA down to 40% of the PGA. This maximum drop would take place for $D/a=2$ and Vs/a about 40.
- Except for $d/D=0$, for almost all other values of d/D, the above conservative trend holds.
- As d/D diminishes, the above conservative trend gradually changes in such a way that for $d/D=0$, $D/a=2$, and $Vs/a=10$, PHIA may reach an amount that is 50% higher than PGA.

In general, having specific value of d/D, higher embedment ratio takes lower PHIAs. This statement has an exception for $d/D=0$ and $D/a=2$.

The averages of normalized PHIAs are summarized in Figure (6). This figure represents the effect of different embedment ratios where the normalized PHIA to PGA is plotted versus Vs/a. Each chart includes four graphs belonging to different states of soil-wall contact lengths. It can be seen that for every embedment ratio, as Vs/a rises, the results
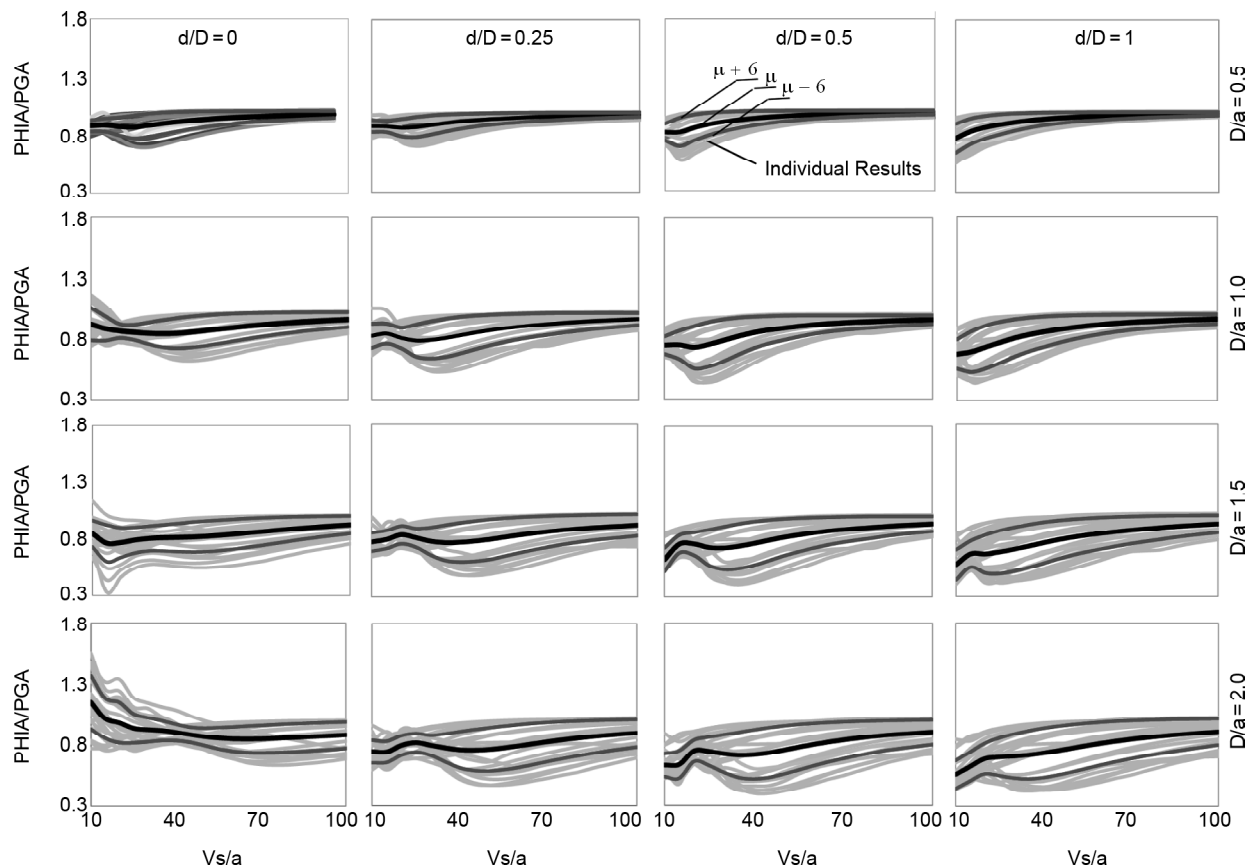
Figure 5. PHIAs normalized to PGAs for selected set of records; Results for individual records in grey style, average results in black and average plus/minus standard deviation in red.
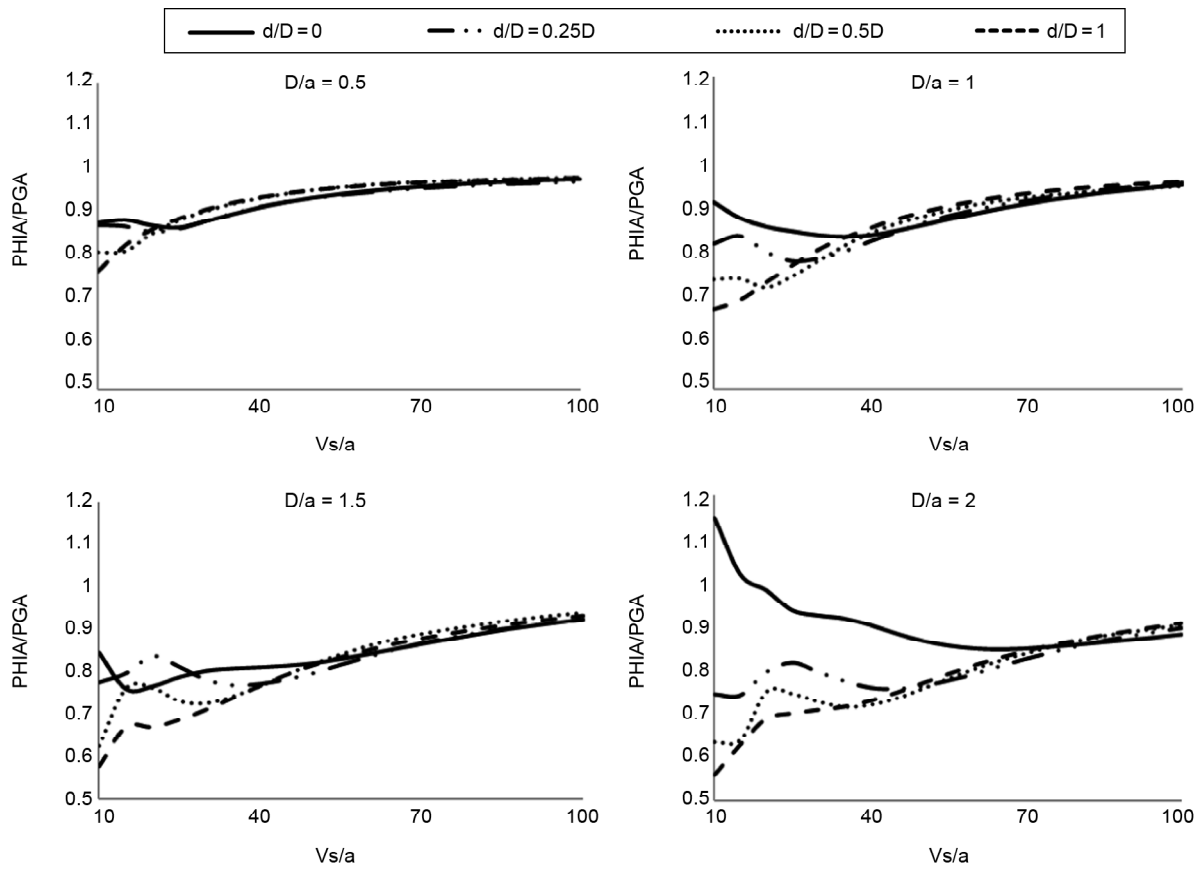
Figure 6. Average values of normalized PHIA arranged by different embedment ratios for various side-wall contact lengths to nearby soil.

for all contact lengths tend to similar values.

Practically, for each specific value of *D/a*, there is a threshold in the abscissa, *Vs/a*, after which PHIAs approaches to same values. The thresholds for *D/a*=0.5, 1, 1.5, and 2 are about 25, 40, 55, and 70 respectively.

To achieve a better understanding of these trends, the charts of Figure (6) are redrawn by different arrangement of dimensionless parameters and depicted in Figure (7). Accordingly, the mentioned averages of PHIAs are displayed by different contact soil-wall states. From Figure (7), it can be found that except for *d/D*=0, the ordinates of PHIA show a sequential grow as *d/D* increases. In the case of *d/D*=0, the above sequence is valid just for value of *Vs/a* above 70. Although lower than that, no regular trend seems to exist.

In order to clarify the dispersion of results for different values of *Vs/a*, a well-known statistical parameter, i.e. covariance, is computed using the ratio of standard deviation to average values. It should be mentioned that lower values for covariance may be interpreted as lower record-dependency

of the results. In another word, for lower values of that statistical parameter, average values of results can better be representatives of general trends.

Summary of this dispersion investigation is presented in Figure (8). Regarding the graphs, usually the more the contact side length to the soil, the more the dispersion is witnessed. Moreover, as the embedment ratio increases from 0.5 to 2, the covariance and hence the record dependency of the results becomes much more notable. For larger embedment ratios, maximum dispersion of the results occurs for larger values of *Vs/a*.

Besides, similar thresholds as was reported in Figure (6) can be followed here. In systems with *Vs/a* beyond such limits, the result dispersions for different side-wall contact lengths, approach approximately to the same values. These milestones for *D/a*=0.5, 1, 1.5 and 2 may be characterised by the values of *Vs/a* about 25, 45, 60 and 90 respectively. Another interesting feature in Figure (8) is about local minimum points. Such points are more distinguishable for larger embedment ratios. Referring to Figure (5), these lowermost points
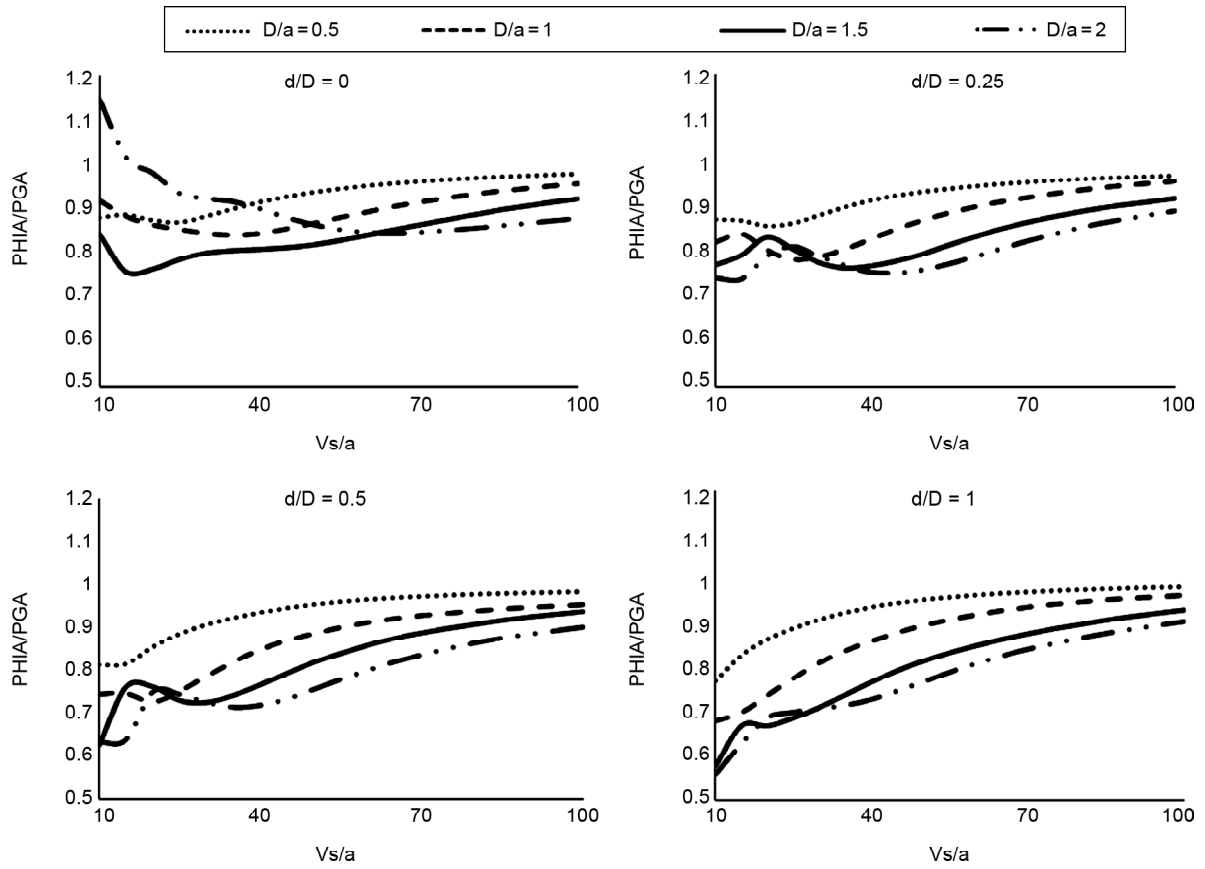
Figure 7. Average values of normalized PHIA arranged by different side wall contact lengths to nearby soil for various embedment ratios.
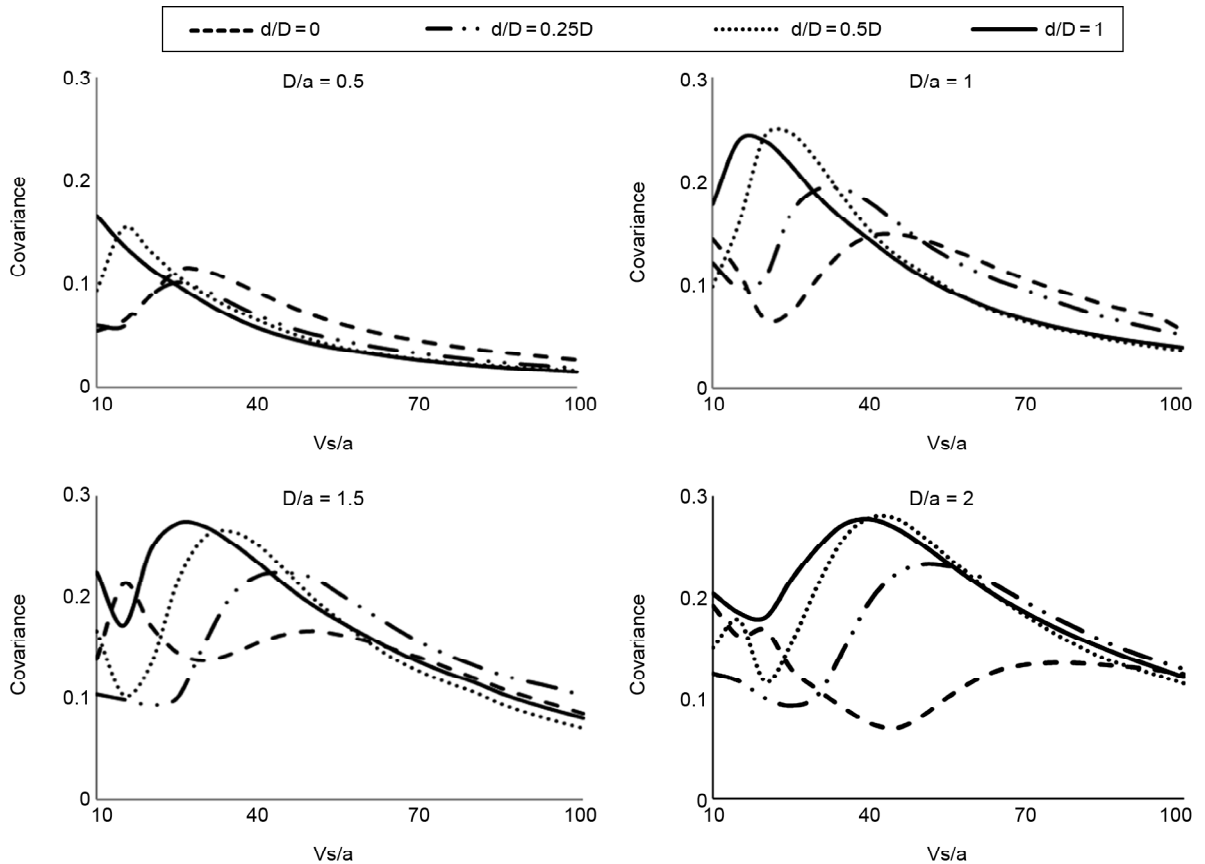

Figure 8. Covariance of PHIAs for different embedment ratios and various side contact lengths to nearby soil.

can be attributed to necking regions of result ensemble. In those districts, reliability of conclusions improves and record dependency of results decreases.

6. Conclusions

A numerical analysis, using finite element method, is conducted to investigate the effect of kinematic interaction on peak horizontal input acceleration, PHIA. The foundation is supposed as 2D rigid strip inclusion in soil with different depths of embedment. In addition, the side-walls are allowed to have incomplete contact to surrounding medium. At first step, KI effects are presented as transfer functions in frequency domain for translational components of input motion. It is concluded that generally KI scale the components of FFM to a fraction of unity. For low frequency ranges, as the contact length decreases, the ordinates of transfer functions take lower values. However, a reverse trend is witnessed for high frequency regions. At the second step, the influence of KI on PHIA is explored. For that purpose, the calculated TFs in previous step are applied to a set of 20 selected records. Then, by inspecting the resulted modified records, PHIAs are sorted against different values of Vs/a. It is figured out that PHIAs are notably affected by KI phenomenon. Such effects are intensified as embedment ratio increases. For the case of full contact with adjacent medium, the effect is almost always conservative. However, as contact length decreases, this conservatism diminishes in such a way that for no contact condition to side medium, PHIA may grow up to 1.5 times of PGA. This point may be important as in current practice usually embedment of foundation would take place. Hence, using PGA as design peak ground acceleration may become, in many cases, very conservative and also sometimes unconservative.

References

1. Bielak, J. (1974) Dynamic behavior of structures with embedded foundations. *Earthquake Engineering and Structural Dynamics*, **3**, 259-274.

2. Iguchi, M. (1982) An approximate analysis of input motion for rigid embedded foundation. *Transactions of Architectural Institute of Japan*, **315**, 61-75.

3. Mori, M. and Fukuwa, N. (2012) Simplified evaluation methods for impedance and foundation input motion of embedded foundation. *Proc. of the 15ᵗʰ World Conf. on Earthquake Engineering*, Lisbon.

4. Pais, A. and Kausel, E. (1985) *Stochastic Response Of Foundations*. Report No. R8506, Massachusetts Institute of Technology, Cambridge, MA.

5. Luco, J.E. (1969) Dynamic interaction of a shear wall with the soil. *Journal of the Engineering Mechanics Division*, **95**(2), 333-346.

6. Trifunac, M. (1972) Interaction of a shear wall with the soil for incident plane SH waves. *Bulletin of the Seismological Society of America*, **62**(1), 63-83.

7. Luco, J.E., Wong, H.L., and Trifunac, M.D. (1975) A note on the dynamic response of rigid embedded foundation. *Earthquake Engineering and Structural Dynamics*, **4**, 119-127.

8. Novak, M.D. and Beredugo, Y.O. (1972) Vertical vibration of embedded footings. *Journal of the Soil Mechanics and Foundation Division*, **98**(12), 1291-1310.

9. Novak, M.D. (1973) *The Effect of Embedment on Vibration of Footings and Structures*. [Synopsis]. Faculty of Engineering Science, University of Ontario, Canada.

10. Hoshiya, M. and Ishii, K. (1983) Evaluation of kinematic interaction of soil-foundation systems by a stochastic model. *Proceedings of the First International Conference and Exhibition on Soft Dynamics and Earthquake Engineering*, Southampton, UK.

11. Iguchi, M. (1984) Earthquake response of embedded foundation to SH and SV wave. *Proceedings of 8th World Conference on Earthquake Engineering*, San Francisco (CA), 1081-1088.

12. Luco, J. and Mita, A. (1987) Response of circular foundation to spatially random ground

motion. *Journal of Engineering Mechanics*, **113**(1), 1-15.

13. Luco, J.E. (1976) Torsional response of structures for SH waves. The case of hemispherical foundations. *Bulletin of Seismological Society of America*, **66**(1), 109-123.

14. Wong, H.L. and Luco, J.E. (1978) Dynamic response of rectangular foundations to obliquely incident seismic waves. *Earthquake Engineering and Structural Dynamics*, **6**, 3-16.

15. Luco, J.E. and Wong, H.L. (1987) Seismic response of foundations embedded in a layered half-space. *Earthquake Engineering and Structural Dynamics*, **15**, 233-247.

16. Mita, A. and Luco, J. (1989a) Dynamic response of a square foundation embedded in an elastic half-space. *Soil Dynamics and Earthquake Engineering*, **8**(2), 54-67.

17. Mita, A. and Luco, J. (1989b) Impedance function and input motion for embedded structures. *Journal of Geotechnical Engineering* (ASCE), **115**(4), 491-503

18. Veletsos, A.S. and Prasad, A.M. (1989) Seismic interaction of structures and soils. *Journal of Structural Engineering* (ASCE), **115**(4), 935-956.

19. Kausel, E., Whitman, R.V., Morray, J.P., and Elsabb, F. (1978) Effects of horizontally travelling waves in soil-structure interaction. *Nuclear Engineering and Design*, **48**, 377-392.

20. Kurimoto, O. and Iguchi, M. (1996) Evaluation of input motion based on observed motion. *Proceedings of the 11th International Conference on Earthquake Engineering*, Acapulco, Mexico.

21. Iguchi, M. (2001) On effective input motions. Observations and simulation analyses. *The 2nd UJNR Workshop on Soil-Structure Interaction*, Tsukuba, Japan.

22. Givens, M.J. and Stewart, J.P. (2012) Assessment of soil-structure interaction modeling strategies for response history analysis of buildings. *Proceedings of the 15th International Conference on Earthquake Engineering*, Lisbon, Portugal.

23. Rayhani, MT. and El Naggar, MH. (2007) Centrifuge modeling of seismic response of layered soft clay. *Bull Earthquake Engineering*, **5**(4), 571-589.

24. Torabi, H. and Rayhani, MT. (2014) Three dimensional finite element modeling of seismic soil-structure interaction in soft soil. *Computers and Geotechnics*, **60**(4), 9-19.

25. ABAQUS Inc. (2011) V.6.11 User's Manual. Providence, Rhode Island, USA.

26. Wang, Y. and Rajapakse, R. (1991) Dynamics of rigid strip foundations embedded in orthotropic Elastic Soils. *Earthquake Engineering and Structural Dynamics*, **20**(3), 927-947.

27. Jahankhah, H., Ghannad, M.A., and Rahmani, M. (2013) Alternative solution for kinematic interaction problem of soil-structure systems with embedded foundation. *The Structural Design of Tall and Special Buildings*, **22**(3), 251-266